

Split of zero-bias conductance peak in normal metal / d-wave superconductor junctions

Yasuhiro A sano

D epartm ent of A ppiled P hysics, H okkaido U niversity, Sapporo 060-8628, Japan

Yukio Tanaka

D epartm ent of A ppiled P hysics, N agoya U niversity, N agoya 464-8603, Japan

Satoshi K ashiiw aya

N ational Institute of A dvanced Industrial Science and Technology, T sukuba, 305-8568, Japan

(D ated: D ecember 18, 2019)

E ffects of impurities on the conductance in normal metal / d-wave superconductor junctions are discussed. By using the single-site approximation, it is shown that the impurity scattering causes the split of the zero-bias conductance peak (ZBCP). The results are consistent with our previous numerical simulations. So far, the split of the ZBCP at the zero magnetic field has been believed to be a strong evidence of the broken time reversal symmetry states at a surface of a high- T_c superconductor. However we conclude that the impurity scattering can be also an origin of the split of the ZBCP. Typical conductance shapes observed in several experiments are explained well by the present theory.

PACS numbers: 74.81.-g, 74.25.Fy, 74.50.+r

I. INTRODUCTION

The zero-energy state (ZES)¹ formed at a surface of superconductors is a consequence of the unconventional symmetry of Cooper pairs. Since the ZES appears just on the Fermi energy, it drastically affects transport properties through the interface of junctions consist of unconventional superconductors². For instance in normal metal / high- T_c superconductor junctions, a large peak is observed in the differential conductance at the zero bias-voltage^{3,4,5,6,7,8,9,10}. The ZES is also responsible for the low-temperature anomaly of the Josephson current between the two unconventional superconductors^{11,12,13,14,15,16}.

An electron incident into a normal metal / superconductor (NS) interface suffers the Andreev reflection¹⁷ by the pair potential in the superconductor. As a result, a hole traces back the original propagation path of the incident electron. This is called the retro property of a quasiparticle which supports the formation of the ZES. Strictly speaking, the electron-hole pairs just on the Fermi energy hold the retro property in the presence of the time reversal symmetry (TRS). Thus the ZES is sensitive to the TRS of the system. Actually, the zero-bias conductance peak (ZBCP) in NS junctions splits into two peaks under magnetic fields^{18,19,20,21}. The peak splitting is also discussed^{22,23,24,25,26,27,28} when the broken time reversal symmetry state (BT RSS) is formed at the interface. Theoretical studies showed that such BT RSS's are characterized by the $s+id$ ²³ or $d+id$ ²⁹ pairing symmetry. Experimental results are, however, still controversial. Some experiments reported the split of the ZBCP at the zero magnetic field^{30,31,32,33,34}, others did not observe the splitting^{5,7,8,35,36,37}. The ZBCP is also sensitive to the exchange potential in ferromagnets attaching to uncon-

ventional superconductors^{38,39}.

In previous papers, we numerically showed that random potentials at the NS interface cause the split of the ZBCP at the zero magnetic field by using the recursive Green function method^{40,41}. We also showed that the splitting due to the impurity scattering can be seen more clearly when realistic electronic structures of high- T_c materials are taken into account⁴². Unfortunately, we could not make clear a mechanism of splitting. Our conclusion, however, contradicts to those of a number of theories^{43,44,45,46,47,48} based on the quasiclassical Green function method^{49,50,51,52,53}. The drastic suppression of the ZBCP by the interfacial randomness is the common conclusion of all the theories. The theories of the quasiclassical Green function method, however, concluded that the random potentials do not split the ZBCP. Thus this issue has not been xed yet. There are mainly two reasons for the disagreement in the two theoretical approaches (i.e., the recursive Green function method and the quasiclassical Green function method). One is the treatment of the random potentials, the other is the effects of the rapidly oscillating wave functions on the conductance. In our simulations, we calculate the conductance without any approximation to the random potentials and the wave functions; this is an advantage of the recursive Green function method^{41,54}.

In this paper, we discuss effects of the impurity scattering on the conductance in normal metal / d-wave superconductor junctions by using the Lippmann-Schwinger equation. We assume that impurities are near the NS interface on the superconductor side. The differential conductance is analytically calculated within the single-site approximation based on the conductance formula^{55,56}. The split of the ZBCP due to the impurity scattering is the main conclusion of this paper. We discuss two energy

scales: (i) $E_{ZEP} = \frac{1}{2} k_F v_F T_B$ characterizing the width of the ZBCP, where T_B is the normal transmission probability of the junction, and (ii) $E_{dip} = \frac{1}{2} k_F v_F = \frac{1}{2} \hbar k_F = \frac{1}{2} \hbar v_F = \frac{1}{2} \hbar k_F m$ characterizing a dip structure of the conductance at the zero bias, where k_F is the Fermi wave number, $\hbar = \hbar v_F = \frac{1}{2} \hbar k_F$ is the coherence length and $v_F = \hbar k_F = m$ is the Fermi velocity. When $eV_{bias} < E_{dip}$, we show that the impurity scattering drastically suppresses the conductance, where V_{bias} is the bias voltage applied to junctions. As a result, a dip structure is seen in the differential conductance. In addition to the dip structure, we also discuss the splitting peaks found at $eV_{bias} < E_{ZEP}$. The impurity scattering affects the conductance in two ways: (i) drastically suppressing the zero-bias conductance and (ii) making the conductance peak wider. The split of the ZBCP is a consequence of these two effects. In the present theory, we successfully explain typical conductance shapes observed in several experiments. We conclude that the split of the ZBCP in the zero magnetic field is not the direct evidence of the BTRS at a surface of high- T_c superconductors.

This paper is organized as follows. In Sec. II, we derive the reaction coefficients in NS junctions within the single-site approximation based on the Lippmann-Schwinger equation. The split of the ZBCP is discussed in Sec. III. In Sec. IV, calculated results are compared with experiments and another theories. In Sec. V, we summarize this paper.

II. LIPPMANN-SCHWINGER EQUATION

Let us consider two-dimensional NS junctions as shown in Fig. 1, where normal metals ($x < 0$) and d-wave superconductors ($x > 0$) are separated by the potential barrier $V_B(r) = V_B(x)$. We assume the periodic boundary condition in the y direction and the width of the junction is W . The x axis of high- T_c superconductors is oriented

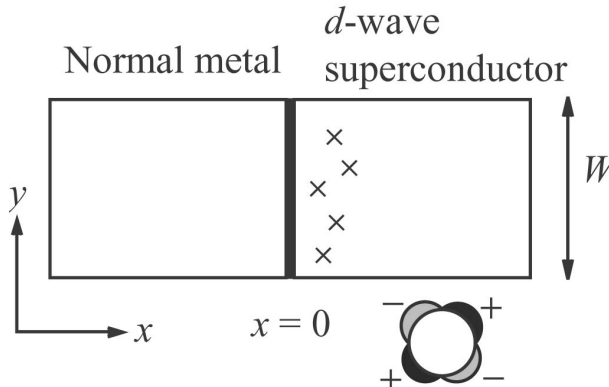


FIG. 1: The normal metal / d-wave superconductor junction is schematically illustrated. The crosses represent impurities.

by the 45 degree from the interface normal. The pair

potential of a high- T_c superconductor is described by

$$k = 2 \frac{1}{2} k_F k_y; \quad (1)$$

in the momentum space, where $k_x = \cos \theta = k_x/k_F$ and $k_y = \sin \theta = k_y/k_F$ are the normalized wave number on the Fermi surface in the x and the y direction, respectively. The schematic figure of the pair potential is shown in Fig. 1. The NS junctions are described by the Bogoliubov-de Gennes equation⁵⁷,

$$\begin{aligned} Z \frac{dr^0}{dr} &= \frac{(r - r^0)h_0(r^0)}{(r; r^0)} \frac{(r; r^0)}{(r - r^0)h_0(r^0)} \\ u(r^0) &= E u(r) \\ v(r^0) &= E v(r); \end{aligned} \quad (2)$$

$$h_0(r) = \frac{\hbar^2 r^2}{2m} + V(r) \quad ; \quad (3)$$

$$V(r) = V_B(r) + V_I(r); \quad (4)$$

$$R_c(r_r) = \begin{cases} \frac{1}{V_{vol}} k_r e^{ik_r r_r} & : X_c > 0 \\ 0 & : X_c < 0 \end{cases}; \quad (5)$$

where $R_c = (X_c; Y_c) = (r + r^0)/2$ and $r_r = r - r^0$. Throughout this paper, we neglect the spatial dependence of the pair potential near the junction interface. This is a reasonable approximation when we consider the conductance around the zero-bias⁵⁸. The spatial dependence of the pair potential should be determined in a self-consistent way when we discussed the conductance far from the zero-bias such as $eV_{bias} \neq 0$.

We consider impurities near the interface on the superconductor side as indicated by crosses in Fig. 1. The potential of impurities is given by

$$V_I(r) = V_i \sum_{j=1}^{N_i} (r - r_j); \quad (6)$$

where N_i is the number of impurities. In the absence of impurities, the transmission and the reaction coefficients are calculated from boundary conditions of wave functions at the junction interface as shown in Appendix A. By using these coefficients, four retarded Green functions are obtained as shown in Appendix B. The normal conductance of the junction is given by

$$G_N = \frac{2e^2}{h} N_c T_B; \quad (7)$$

$$T_B = \frac{2}{d} \int_0^d \frac{\cos^3}{z_0^2 + \cos^2}; \quad (8)$$

where T_B is the transmission probability of the junction, $N_c = 2W = \frac{1}{2} k_F$ is the number of the propagating channels on the Fermi surface, $\frac{1}{2} k_F = \frac{1}{2} \hbar k_F$ is the Fermi wave length and $z_0 = m V_B = (\hbar^2 k_F)^2$ represents the strength of the potential barrier at the NS interface. In the limit of $z_0^2 \ll 1$, T_B is proportional to $1/z_0^2$.

Effects of impurities on the wave functions are taken into account by using the Lippmann-Schwinger equation,

$$^{(1)}(\mathbf{r}) = \hat{\psi}_0^{(1)}(\mathbf{r}) + \int d\mathbf{r}' \hat{G}_0(\mathbf{r}; \mathbf{r}') V_1(\mathbf{r}') \hat{\psi}_3^{(1)}(\mathbf{r}'); \quad (9)$$

$$= \hat{\psi}_0^{(1)}(\mathbf{r}) + \sum_{j=1}^{N_i} \hat{G}_0(\mathbf{r}; \mathbf{r}_j) V_1 \hat{\psi}_3^{(1)}(\mathbf{r}_j); \quad (10)$$

where 1 indicates a propagating channel characterized by the transverse wave number $k_y^{(1)}$. Here $\hat{\psi}_0^{(1)}(\mathbf{r})$ is the wave function in which an electron-like quasiparticle with $k_y^{(1)}$ is incident into the NS interface from normal metals and is described as

$$\begin{aligned} \hat{\psi}_0^{(1)}(\mathbf{r}) = & \hat{\psi}_1(y) \begin{pmatrix} 1 & 0 \\ 0 & 1 \end{pmatrix} e^{i\mathbf{q}_1^+ \cdot \mathbf{x}} + \begin{pmatrix} 0 & 1 \\ 1 & 0 \end{pmatrix} e^{i\mathbf{q}_1^- \cdot \mathbf{x}} \hat{\psi}_{NN}^{he}(1) \\ & + \begin{pmatrix} 1 & 0 \\ 0 & 1 \end{pmatrix} e^{i\mathbf{q}_1^+ \cdot \mathbf{x}} \hat{\psi}_{NN}^{ee}(1); \end{aligned} \quad (11)$$

$$\hat{\psi}_1(y) = \frac{e^{ik_y^{(1)}y}}{W}; \quad (12)$$

for $x < 0$, where $\mathbf{q}_1^+ = \frac{p}{k_1^2 - k_F^2} \mathbf{E} = \mathbf{E}_F$ is the wave number of a quasiparticle in normal metals and $k_1^2 + k_y^{(1)2} = k_F^2$. For $x > 0$, the wave function is given by

$$\begin{aligned} \hat{\psi}_0^{(1)}(\mathbf{r}) = & \hat{\psi}_1(y) \begin{pmatrix} u_1 & 0 \\ v_1 & 1 \end{pmatrix} e^{i\mathbf{q}_1^+ \cdot \mathbf{x}} \hat{\psi}_{SN}^{he}(1) \\ & + \begin{pmatrix} v_1 & 0 \\ u_1 & 1 \end{pmatrix} e^{i\mathbf{q}_1^- \cdot \mathbf{x}} \hat{\psi}_{SN}^{ee}(1); \end{aligned} \quad (13)$$

$$u_1 = \frac{r}{\frac{E + \frac{1}{2}}{2E}}; \quad (14)$$

$$v_1 = \text{sgn}(k_y^{(1)}) \frac{E - \frac{1}{2}}{2E}; \quad (15)$$

where $k_1 = k_1^2 - k_F^2 = \frac{p^2}{E^2 - \frac{1}{4}}$ is the wave number of a quasiparticle in superconductors, $\hat{\psi}_1 = \frac{p}{E^2 - \frac{1}{4}}$ and $\hat{\psi}_1 = 2 \hat{\psi}_0 k_1 k_y^{(1)}$. The wave function at an impurity $\hat{\psi}_0^{(1)}(\mathbf{r}_{j0})$ can be obtained by $\mathbf{r} \neq \mathbf{r}_{j0}$ in Eq. (10)

$$\hat{\psi}_0^{(1)}(\mathbf{r}_{j0}) = \sum_{j=1}^{N_i} \hat{\psi}_0^{(1)}(\mathbf{r}_{j0}) \hat{G}_0^{ss}(\mathbf{r}_{j0}; \mathbf{r}_j) V_1 \hat{\psi}_3^{(1)}(\mathbf{r}_j); \quad (16)$$

In the single-site approximation, the multiple scattering by an impurity is fully taken into account and that involving many impurities are neglected. In the summation of j in Eq. (16), only the contribution with $j = j_0$ is taken into account in the single-site approximation⁵⁹. In this way, the wave function at \mathbf{r}_j is approximately given by

$$\hat{\psi}_0^{(1)}(\mathbf{r}_j) = \hat{\psi}_0^{(1)} \hat{G}_0^{ss}(\mathbf{r}_j; \mathbf{r}_j) V_1 \hat{\psi}_3^{(1)} \hat{\psi}_0^{(1)}(\mathbf{r}_j); \quad (17)$$

We note that the single-site approximation yields the exact results when $N_i = 1$. Within the single-site approximation, Eq. (10) can be solved as

$$\begin{aligned} \hat{\psi}_{SSA}^{(1)}(\mathbf{r}) = & \hat{\psi}_0^{(1)}(\mathbf{r}) + \sum_{j=1}^{N_i} \hat{G}_0^{NS}(\mathbf{r}; \mathbf{r}_j) V_1 \hat{\psi}_3^{(1)} \\ & + \hat{G}_0^{ss}(\mathbf{r}_j; \mathbf{r}_j) V_1 \hat{\psi}_3^{(1)} \hat{\psi}_0^{(1)}(\mathbf{r}_j); \end{aligned} \quad (18)$$

for $x < 0$.

In the presence of the impurity scattering, the wave function Eq. (18) can be expressed as

$$\begin{aligned} \hat{\psi}_{SSA}^{(1)}(\mathbf{r}) = & \begin{pmatrix} 1 & 0 \\ 0 & 1 \end{pmatrix} \hat{\psi}_1(y) e^{i\mathbf{q}_1^+ \cdot \mathbf{x}} \\ & + \begin{pmatrix} X & 0 \\ 0 & 1 \end{pmatrix} \hat{\psi}_1(y) e^{i\mathbf{q}_{10}^- \cdot \mathbf{x}} A_{10;1} + \begin{pmatrix} 1 & 0 \\ 0 & 1 \end{pmatrix} e^{i\mathbf{q}_{10}^+ \cdot \mathbf{x}} B_{10;1}; \end{aligned} \quad (19)$$

for $x < 0$, where $A_{10;1}$ and $B_{10;1}$ are the Andreev and the normal reflection coefficients, respectively. These coefficients are obtained from relations

$$Z_{W=2} \frac{dy}{d\mathbf{y}} \hat{\psi}_m(y)(0;1) \hat{\psi}_{SSA}^{(1)}(\mathbf{r}) = e^{i\mathbf{q}_m \cdot \mathbf{x}} A_{m;1}; \quad (20)$$

$$Z_{W=2} \frac{dy}{d\mathbf{y}} \hat{\psi}_m(y)(1;0) \hat{\psi}_{SSA}^{(1)}(\mathbf{r}) = e^{i\mathbf{q}_m^+ \cdot \mathbf{x}} \hat{\psi}_{1m} + e^{i\mathbf{q}_m^+ \cdot \mathbf{x}} B_{m;1}; \quad (21)$$

In what follows, we consider low transparent junctions, (i.e., $z_0^2 \ll 1$). From the reflection coefficients in Appendix A, the Green function in the superconductor is given by

$$\begin{aligned} \hat{G}_0^{ss}(\mathbf{r}; \mathbf{r}) = & i N_0 \frac{2}{z_0^2} \int_0^Z d\mathbf{r}' \frac{E}{2} \hat{\psi}_0^{(1)} \frac{z_0^2}{2} \frac{f_1}{k} \frac{\cos(2k_F \cdot \mathbf{x} \cos \phi) g e^{2ipx}}{2} \hat{\psi}_0^{(1)} \\ & \frac{z_0^2 E}{2} \frac{E}{2} \cos(2k_F \cdot \mathbf{x} \cos \phi) \hat{\psi}_0^{(1)} + i \sin(2k_F \cdot \mathbf{x} \cos \phi) \hat{\psi}_3^{(1)} e^{2ipx} \frac{\frac{2}{k} \cos^2 \frac{E^2}{4} e^{2ipx}}{i} \hat{\psi}_0^{(1)} \\ & \frac{z_0 \cos \phi}{2} e^{2ipx} f E \cos(2k_F \cdot \mathbf{x} \cos \phi) \hat{\psi}_3^{(1)} + i \sin(2k_F \cdot \mathbf{x} \cos \phi) \hat{\psi}_0^{(1)} g; \end{aligned} \quad (22)$$

where $p = \frac{k_F}{2 \cos \frac{x}{k_F}}$: The local density of states at r is defined by

$$N_s(E; x) = -\frac{1}{2} \operatorname{Im} \operatorname{Tr} \hat{G}_0^{SS}(r; r); \quad (23)$$

The 1st term in Eq. (22) contributes to the bulk density of states. Since $2p$ is roughly estimated to be $1 = 0$, other terms contribute to the local density of states near the interface. In low transparent junctions, 6th, 7th and 8th terms are negligible. The 4th and the 5th terms are also negligible because integrals of such rapidly oscillating functions become very small. The 2nd and 3rd terms are dominant for $E = 0$. In Fig. 2, we show the Green function in Eq. (22) as a function of E , where $z_0 = 5$, $\epsilon_0 = 0.1 \mu_F$, $xk_F = 5$, and $N_0 = m = (h^2)$ is the normal density of states in the unit area. Since $xk_F = 7$, the results correspond to the Green function at a distance 0 away from the interface. The two energy scales in Fig. 2 are defined by

$$E_{ZEP} = \frac{0}{z_0^2}; \quad (24)$$

$$E_{dip} = \frac{0}{z_0^2 (xk_F)^3}; \quad (25)$$

The horizontal axes are normalized by E_{ZEP} and E_{dip} in (a) and (b), respectively. The solid and the broken lines represent negative of the imaginary part and the real part of Eq. (22), respectively. As shown in (a) and

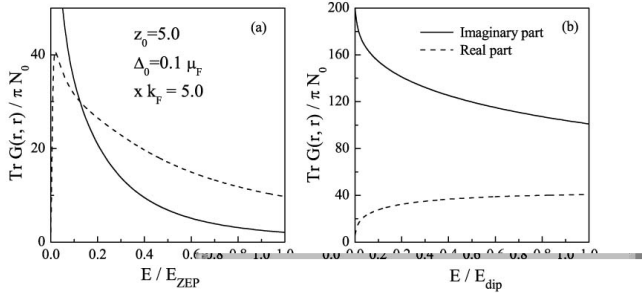


FIG. 2: The Green function in the superconductor is shown as a function of E , where $z_0 = 5$, $xk_F = 5$ and $\epsilon_0 = 0.1 \mu_F$. The two energy scales of the horizontal axes in (a) and (b) are defined by $E_{ZEP} = z_0^2$ and $E_{dip} = z_0^2 (xk_F)^3$, respectively.

(b), the imaginary part of the Green function has a large peak around $E = 0$ reflecting the ZES formed at the junction interface. The energy scale, E_{ZEP} , characterizes the width of the zero energy peak. In (b), the imaginary part (real part) of the Green function rapidly increases (decreases) with decreasing E for $E < E_{dip}$. The Green function for $E < E_{ZEP}$ is approximately calculated from

the 2nd and the 3rd terms of Eq. (22)

$$\hat{G}_0^{SS}(r; r) = \frac{2}{Z} \sum_{n=0}^{\infty} \frac{N_0 z_0^2 e^{xk_F n}}{E^2 z_0^4 + \frac{2}{3} \cos^6 n \sin^2 n}; \quad (26)$$

$$g_1 = \frac{2}{Z} \sum_{n=0}^{\infty} \frac{\cos^4 n \sin^2 n \sin^2(xk_F \cos n)}{E^2 z_0^4 + \frac{2}{3} \cos^6 n \sin^2 n}; \quad (27)$$

$$g_2 = \frac{2}{Z} \sum_{n=0}^{\infty} \frac{E z_0^2 \cos n \sin n \sin^2(xk_F \cos n)}{E^2 z_0^4 + \frac{2}{3} \cos^6 n \sin^2 n}; \quad (28)$$

where we use $i \frac{\partial}{\partial x} \cos n \sin n$. The imaginary part of the Green function, g_1 , is of the order of unity when $E = E_{ZEP}$. However, g_1 at $E = 0$ becomes much larger than unity for $xk_F \ll 1$ because

$$g_1(E = 0) = \frac{2}{Z} \sum_{n=0}^{\infty} \frac{\sin^2 n xk_F \cos n}{\cos^2 n} \approx xk_F; \quad (29)$$

Thus the energy scale, E_{dip} , characterizes the drastic increase of g_1 and the drastic decrease of g_2 . The local density of states at $E = 0$ is plotted as a function of xk_F in Fig. 3 with the solid line. For comparison, we also show the analytical results represented by

$$\operatorname{Im} \hat{G}_0^{SS}(r; r) \Big|_{E=0} = 2 N_0 z_0^2 e^{xk_F} \approx xk_F; \quad (30)$$

with the broken line. The results show the remarkable enhancement of the local density of states around $xk_F = 0$. This implies that the ZES is formed around $xk_F = 0$.

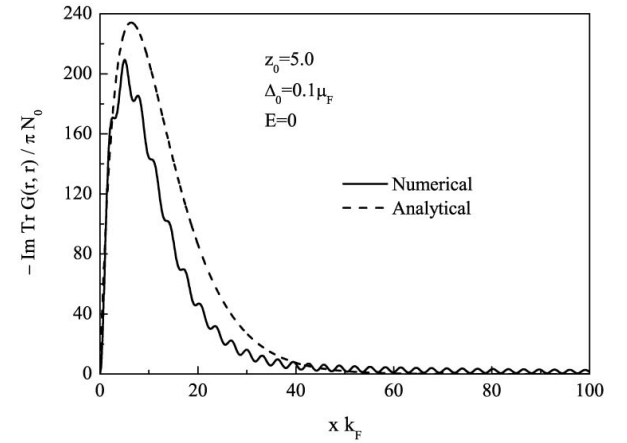


FIG. 3: The imaginary part of the Green function is shown as a function of xk_F , where $E = 0$, $z_0 = 5$ and $\epsilon_0 = 0.1 \mu_F$. The numerical and the analytical results are denoted by the solid and the broken lines, respectively.

Here we note several remarks as follows. To calculate the Green function, we consider the 3rd term in Eq. (22) which rapidly oscillates as $\cos(2xk_F \cos n)$. Such rapidly oscillating terms are usually neglected in the quasiclassical Green function method. We cannot neglect the 3rd

term, however, because it removes the divergence of the local density of state at $E = 0$ ^{60,61}. The 3rd term also becomes important when we calculate the local density of states just at the surface, (i.e., $x = 0$),

$$\frac{N_s(E;0)}{N_0} = \text{Re} \int_0^Z \frac{d}{dE} \frac{2E^2 z_0^2 + \frac{2}{k} \cos^2}{2} ; \quad (31)$$

$$, \frac{2}{K} \frac{z_0}{E} + \frac{2}{0} \int_0^Z \frac{d}{dE} \frac{E^2 z_0^2 + \frac{2}{0} \cos^6 \sin^2}{E^2 z_0^4 + \frac{2}{0} \cos^6 \sin^2} ; \quad (32)$$

where $K(x)$ is the complete elliptic integral of the first kind and describes the bulk density of states. Another term comes from the 4th and 6th terms in Eq. (22). The first equation is the exact expression and we use $E < E_{ZEP}$ in the second line. We exactly obtain $N_s(E = 0; x = 0) = N_0$. Thus there is no remarkable enhancement in the zero energy local density of states just at the interface. The 2nd and the 3rd terms in Eq. (22) do not contribute to the $N_s(E;0)$ because they exactly cancel with each other at $x = 0$.

In the next section, the conductance for $E < E_{ZEP}$ will be discussed. It is possible to rewrite a part of Eq. (18) as

$$\frac{h}{N_0} V_i G_0^{SS}(r; r) = \frac{i_1}{1 - s^2} ; \quad (33)$$

$$s_1 = Q_0 g_1 ; \quad (34)$$

$$s_2 = Q_0 g_2 ; \quad (35)$$

$$Q_0 = 2 V_i N_0 z_0^2 e^{-x=0} ; \quad (36)$$

$$s = s_2 - i_1 ; \quad (37)$$

where s corresponds to the self-energy of a quasiparticle scattered by an impurity once and describes two important features. First, s becomes large in low transparent junctions even if $V_i N_0$ is fixed at a small constant because Q_0 in Eq.(36) is proportional to $V_i N_0 z_0^2$. $V_i N_0 = T_B$. This behavior explains the previous numerical simulation⁴⁰. Second, effects of impurity scattering far away from the interface on the conductance is negligible because Q_0 decreases exponentially with the increase of x . Impurities around the ZES formed at $x = 0$ seriously affect the conductance for $E < E_{ZEP}$.

III. CONDUCTANCE

The differential conductance in NS junctions is calculated from the normal and the Andreev reflection coefficients,

clients,^{55,56}

$$G_{NS} (eV_{bias} = E) = \frac{2e^2}{h} \int_{-L_m}^{L_m} \frac{1}{k_m} \frac{B_m;1^j + A_m;1^j}{k_m} ; \quad (38)$$

$$A_m;1 = \frac{r}{k_m} A_m;1 ; \quad (39)$$

$$B_m;1 = \frac{r}{k_m} B_m;1 ; \quad (40)$$

When $z_0^2 = 1$ and $E < E_{ZEP}$, the reflection coefficients are calculated as

$$A_m;1 = \int_{-L_m}^{L_m} r_{NN}^{he}(l) + e^{i' L_m;1} [l_m j_1 j(s+1) + l_j m j(s-1)] ; \quad (41)$$

$$B_m;1 = \int_{-L_m}^{L_m} r_{NN}^{ee}(l) + i L_m;1 [j_m j_1 j(s+1) + l_m (s-1)] ; \quad (42)$$

$$L_m;1 = \frac{N_0 V_i z_0^2}{(1 - s^2) k_F} \sum_{j=1}^3 l(Y_j) m(Y_j) \int_{-L_m}^{L_m} \frac{k_m k_m}{1 - m} e^{i(p_m + p_j)x_j} \sin(k_m x_j) \sin(k_l x_j) ; \quad (43)$$

The conductance is then given by

$$G_{NS} = \frac{2e^2}{h} 4 N_c g^{(0)} \sum_{j=1}^3 ; \quad (44)$$

$$g^{(0)} = 2 \int_0^Z \frac{2 \cos^7 \sin^2}{d(E^2 z_0^4 + \frac{2}{0} \cos^6 \sin^2)} ; \quad (45)$$

$$j = R e \frac{s Q_0 (2 I_2 - i I_1 + i I_3)}{s^2 - 1} ; \quad (46)$$

$$I_1 = \frac{2}{0} \int_0^Z \frac{4 \cos^{10} \sin^4 \sin^2(x_j k_F \cos)}{d(E^2 z_0^4 + \frac{2}{0} \cos^6 \sin^2)^2} ; \quad (47)$$

$$I_2 = \frac{2}{0} \int_0^Z \frac{E z_0^2 \frac{3}{0} \cos^7 \sin^3 \sin^2(x_j k_F \cos)}{d(E^2 z_0^4 + \frac{2}{0} \cos^6 \sin^2)^2} ; \quad (48)$$

$$I_3 = \frac{2}{0} \int_0^Z \frac{E^2 z_0^4 \frac{2}{0} \cos^4 \sin^2 \sin^2(x_j k_F \cos)}{d(E^2 z_0^4 + \frac{2}{0} \cos^6 \sin^2)^2} ; \quad (49)$$

The first term of Eq. (44), $N_c g^{(0)}$, is the conductance in clean junctions and j represents effects of the impurity scattering on the conductance. When we calculate $A_m;1^j$ and $B_m;1^j$, the summation with respect to impurities j must be carried out only for $j^0 = j$ in the single-site approximation⁵⁹. As a consequence, the current conservation law is satisfied for $E < E_{ZEP}$. We note that the conductance in Eq. (44) depends on the number of impurities but does not depend on the density of impurities. This is a characteristic behavior of the conductance in the quasi-ballistic regime. Thus the conductance is not described by physical values such as the

mean free path and the mean free time which characterize the conductance in the diffusive regime.

To study effects of impurities on the conductance, we assume $x_j = x_0$ for all impurities. The conductance is rewritten as

$$G_{NS} = \frac{2e^2}{h} N_c g^{(0)} \frac{1}{2n_i} ; \quad (50)$$

where $n_i = N_i N_F = W$ is the dimensionless line density of impurities less than unity. The conductance in Eq. (50) can be characterized by the line density of impurities only when $x_j = x_0$ is assumed for all impurities. When scattering effects are strong, $\beta_j \ll 1$, n_i cannot be much larger than $W = N_F$. This limits the applicability of the single-site approximation. In Fig. 4 (a), we show the conductance as a function of $E = E_{ZEP}$ for several choices of $x_0 k_F$, where $V_i N_0 = 0.01$, $z_0 = 10$ and $n_i = 0.9$. The graph is symmetric with respect to $E = 0$. The broken line indicates the conductance in clean junctions. In

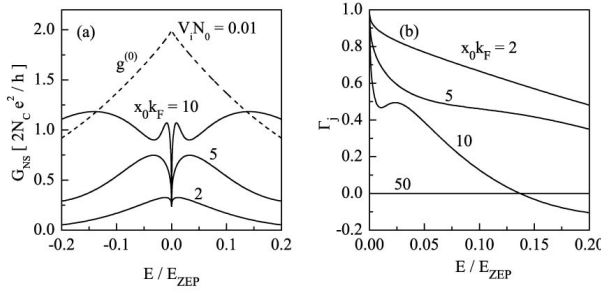


FIG. 4: The conductance is plotted as a function of $E = E_{ZEP}$ in (a), where $V_i N_0 = 0.01$. The function β_j is shown in (b).

(b), β_j is plotted as a function of E . The conductance for all $x_0 k_F$ show a narrow dip at $E = 0$ as shown in (a). This is because β_j rapidly increases with decreasing E for $E < E_{dip}$ as shown in (b). The conductance for $x_0 k_F = 10$ has a complicated structure around $E = 0$ since β_j is not a monotonic function of E as shown in (b). When $E > 0.15 E_{ZEP}$, β_j for $x_0 k_F = 10$ becomes negative and impurities enhance the conductance. As a consequence, the conductance peak becomes wider than $g^{(0)}$. It is impossible to distinguish the conductance for $x_0 k_F = 50$ from $g^{(0)}$ in this plot because β_j for $x_0 k_F = 50$ is almost zero as shown in (b). The impurities far away from the interface, (i.e., $x_0 \gg 10$), do not affect the conductance because Q_0 becomes almost zero as shown in Eq.(36). From these results, we conclude that the conductance has the dip structure $E < E_{dip}$ because of the rapid increase of the local density of states. Since impurities near the interface (i.e., $x_j \ll 10$) contribute to the scattering of a quasiparticle, $\beta_j = (z_0^2)^{3/2} k_F^3$ approximately replaces E_{dip} . Generally speaking, however, E_{dip} is very small energy scale. Thus it seems to be difficult to find

the dip structure for $E < E_{dip}$ in experiments at finite temperatures.

In addition to the dip structure, we find another conductance peaks at $E < E_{ZEP}$. We show several examples in Fig. 5(a)-(c), where $x_0 k_F = 10$, $V_i N_0 = 0.01$ in (a), $x_0 k_F = 20$, $V_i N_0 = 0.005$ in (b) and $x_0 k_F = 260$, $V_i N_0 = 0.1$ in (c). The conductance in (a)-(c) clearly show the peak splitting. The impurity scattering effects

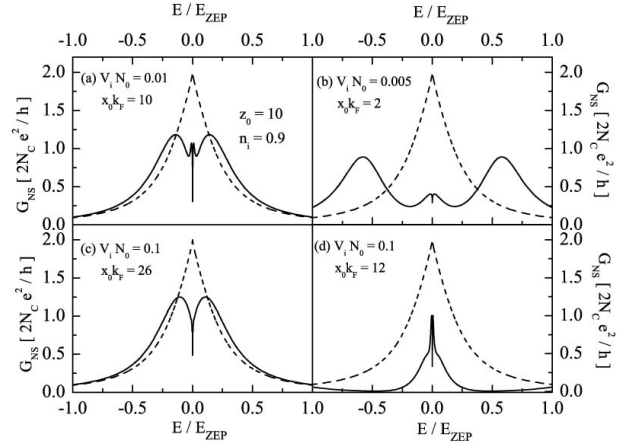


FIG. 5: The conductance is plotted as a function of $E = E_{ZEP}$, where $z_0 = 10$ and $n_i = 0.9$. The parameters are $x_0 k_F = 10$, $V_i N_0 = 0.01$ in (a), $x_0 k_F = 20$, $V_i N_0 = 0.005$ in (b), $x_0 k_F = 26$, $V_i N_0 = 0.1$ in (c) and $x_0 k_F = 12$, $V_i N_0 = 0.1$ in (d). The broken lines denote the conductance in clean junctions.

the ZBCP in two ways: (i) it decreases the zero-bias conductance and (ii) it makes the ZBCP wider. The suppression of the zero-bias conductance is explained in terms of the drastic increase of s_1 which is proportional to the local density of states as shown in Fig. 2. The sign of β_j explains the effect of (ii). For $E_{dip} < E < E_{ZEP}$, β_j is almost a decreasing function of E and is positive at $E = E_{dip}$ as shown in Fig. 4. In the case of $\beta_j < 0$, impurities enhance the conductance and make the ZBCP wider. As a result, the ZBCP splits into two peaks. Therefore the sign change of β_j explains the split of the ZBCP. It is followed from Eq. (46) that

$$\beta_j / \beta_j^2 f s_1 (I_1 - I_2) + 2I_2 s_2 g + f s_1 (I_1 - I_2) = 2I_2 s_2 g; \quad (51)$$

Within our study, $s_1 (I_1 - I_2)$ tends to much smaller than $2I_2 s_2$ for $E_{dip} < E < E_{ZEP}$, which implies an importance of the real part of the self-energy, s_2 , for the splitting. The sign change of β_j happens when

$$\beta_j^2 = s_1^2 + s_2^2 - 1; \quad (52)$$

is satisfied. When $\beta_j (E = E_{dip})$ is a small value less than unity, the effects of impurities are negligible and the conductance almost remains unchanged from that

in clean junctions. The split also cannot be seen when $j_s(E = E_{ZEP})j$ is larger than unity. An example is shown in Fig. 5(d), where $x_0 k_F = 12.0$, $V_i N_0 = 0.1$ and $j_s(E = E_{ZEP})j$ is estimated to be 1.5. The conductance is always smaller than that in clean junctions. As shown in Fig. 5, the magnitude of the impurity potential and the position of impurities are key factors for the degree of splitting. In Fig. 6, the gray area indicates sets of $(V_i N_0; x_0 k_F)$ which satisfy Eq. (52) within $E_{dip} < E < E_{ZEP}$. The open circles denote sets of $(V_i N_0; x_0 k_F)$, where we find the split of the ZBCP in Eq. (50). All the circles are inside of the gray area.

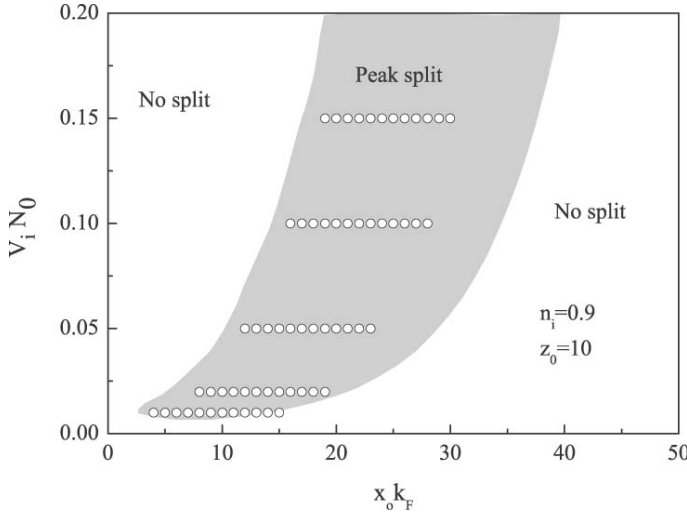


FIG. 6: A phase diagram for the split of the ZBCP. The gray area indicates sets of $(V_i N_0; x_0 k_F)$ which satisfy Eq. (52). The open circles denote sets of $(V_i N_0; x_0 k_F)$, where we find the split of the ZBCP in Eq. (50).

Although the circles and the gray region are not perfectly coincide with each other, they show qualitatively the same tendency. Since Q_0 is proportional to $z_0^2 T_B^{-1}$, the diagram would be changed depending on the transmission probability of junctions.

In Fig. 5, all impurities are aligned at $x_j = x_0$. In real junctions, however, impurities may be distributed randomly near the interface as shown in Fig. 1. The conductance in such realistic junctions are shown in Fig. 7, where impurities are distributed randomly in the range of $1 < x_j k_F < L_s k_F$, $i = N_i \frac{e}{L_s}$ is the dimensionless area density of impurities and $z_0 = 10$. The conductance is calculated from an expression

$$G_{NS} = \frac{2e^2}{h} N_c g^{(0)} + \frac{k_F L_s}{i} h_i ; \quad (53)$$

$$h_i = \frac{1}{N_i} \sum_{j=1}^{N_i} \frac{x_j}{L_s} ; \quad (54)$$

where h_i represents the ensemble average. Since the conductance in Eq. (44) cannot be well characterized

by the impurity density, a factor $k_F L_s$ appears in Eq. (53). We choose $L_s k_F = 20$ in Fig. 7 because $x_0 k_F = 7$. There is no peak splitting for $V_i N_0 = 0.1$ in (a) because most impurities are outside of the gray region in Fig. 6. On the other hand, the results for $V_i N_0 = 0.02$ show the split of the ZBCP because most impurities are inside of the gray region in Fig. 6. The calculated results

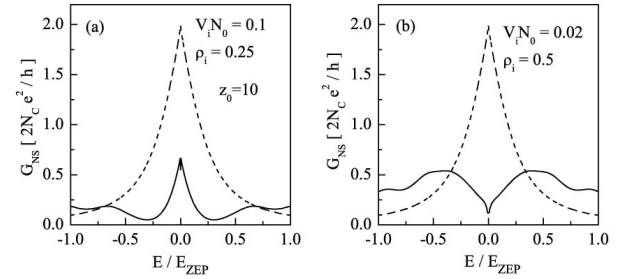


FIG. 7: The conductance in the presence of impurities distributed randomly in the range of $1 < x_j k_F < 20$. The broken lines are the conductance in clean junctions and i is the dimensionless area density of impurities near the interface.

indicate that the strong random potentials are not necessary for the split of the ZBCP. High density impurities with weak random potential are responsible for the split of the ZBCP in low transparent junctions.

Finally we emphasize a similarity in the shapes of the conductance in the present theory and those in experiments. Amazingly, the conductance structure in Fig. 5 (a) is very similar to that observed in the experiment³⁰. It is possible to find a very small conductance peak at $V_{bias} = 0$ in addition to the splitting peaks around $V_{bias} = 1mV$ in Fig. 2 of Ref.30. Almost the same structure is found in the conductance in Fig. 5(b). The impurities away from the interface explains another conductance shape in the experiment⁸. The conductance structure in Fig. 2 of Ref. 8 is very similar to that in Fig. 5 (d). The present theory explains, at least, two typical conductance shapes observed in the experiments. Thus we conclude that the split of the ZBCP in zero-magnetic field is not the direct evidence of the BTRS at a surface of high- T_c superconductors.

IV. DISCUSSION

In experiments, the split of the ZBCP has been reported in overdoped high- T_c superconductors³³. The heavy carrier doping may bring a number of defects or imperfections in superconductors. It is evident that the impurity scattering is unavoidable even in underdoped high- T_c superconductors. The split of the ZBCP would be found in underdoped superconductors if they have bad

sample quality. In the same way, the split of the ZBCP would not be found even in overdoped superconductors if their sample quality are good enough. The sample quality is a key factor for the split of the ZBCP. This argument is consistent with an experiment⁶², where the potential disorder is artificially introduced to the NS junctions by the ion-irradiation and washes out the ZBCP in the limit of strong disorder.

In order to compare the theoretical results in this paper with experiments, we may consider the impurity scattering in normal metals. The total resistance (R) in the dirty normal metal / (110) d-wave junction can be described simply by $R = R_D + R_{NS}$ ⁶³, where $R_D = 1 = G_D$ is the resistance of the dirty normal metal and $G_{NS} = 1 = R_{NS}$ is the conductance discussed in this paper. The equation indicates the absence of the proximity effect in the dirty normal metal^{64,65}. The height of the ZBCP can be reduced to reasonable values in the presence of the impurity scattering in normal metals because the total conductance is given by $1 = (R_D + R_{NS})$. The degree of splitting depends on parameters such as the potential of impurities (V_j), the position of impurities (x_j) and the transparency of the junction ($T_B = 1 = z_0^2$). In particular, T_B is the most important parameter. As shown in Figs. 5 and 7, the degree of splitting is roughly given by $E_{ZEP} = z_0^2 = T_B$. Thus it is possible to choose T_B to fit the degree of splitting with that found in experiments. The amplitude of the pair potential is about 30-40 m eV in typical high- T_c materials. The degree of splitting is then estimated to be 1.2-1.6 m eV for $z_0 = 5$, which is almost consistent with that found in experiments, for instance, 2 m eV³⁰. It is also necessary to consider electronic structures of high- T_c materials for the quantitative agreement of the splitting width in theories with that in experiments.

In quasiclassical Green function theories, the conductance is proportional to the density of states at the surface of superconductors. We find that E dependence of the density of states at the interface in Eq. (32) is apparently different from that of the conductance even in the clean junctions shown in Eq. (45). We also find that $N_s(E; x = 0) = N_0 = N_s(E; x = \infty)$ as shown in Fig. 3. The density of states near the interface averaged over ω in this paper may corresponds to the surface density of states in the quasiclassical approximation, where the rapidly oscillating part of the wave function are neglected and the smallest length scales is given by ω . It is impossible to directly compare the present theory with the quasiclassical Green function theories because the position of impurities is a key parameter for the split of the ZBCP in our theory.

The Abrikosov-Gorkov (AG) theory⁶⁶ is a useful approach to discuss the impurity scattering in superconductors. The applicability of the AG theory is limited to the superconductivity in diffusive metals, where the mean free path is much smaller than the size of the disordered region in superconductors. Here we briefly discuss a relation between the AG theory and ours. Since the AG

theory assumes the diffusive transport regime, we define the mean free path of a quasiparticle in the Born approximation,

$$\gamma = v_F \quad ; \quad (55)$$

$$\frac{h}{\gamma} = 2 \cdot \frac{N_0 V_i^2}{L_s}; \quad (56)$$

$$i = N_i = W \cdot L_s; \quad (57)$$

where we consider $W = L_s$ disordered region on two-dimensional superconductor as in Fig. 7. The impurity density i can be replaced by the dimensionless impurity density $i = (2 = k_F)^2 \cdot i$. The ratio of the mean free path and the coherence length is given by

$$\frac{\gamma}{\lambda} = \frac{0}{F} \frac{0}{N_0 V_i^2} \quad (58)$$

In this paper, γ_0 is larger than unity even in the limit of $i = 1$ because we assume $\gamma_0 = F = 0.1$ and $N_0 V_i < 0.1$. On the other hand, the dirty limit is defined by a relation $\gamma_0 = 1$. When we choose L_s being a few coherence length as shown in Fig. 7, where $L_s = 3_0$, we find that γL_s is still larger than unity. The disordered region is not in the diffusive regime but in the quasi-ballistic regime because the diffusive regime is characterized by a relation $\gamma L_s = 1$. Thus it is basically impossible to apply the Abrikosov-Gorkov theory to the model in this paper. The scattering theory⁵⁹ used in this paper is a suitable analytic method to discuss the conductance of such NS junctions. Although the impurity scattering near the interface is very weak in normal states, it drastically affects the conductance below the critical temperature. Impurities located at the resonant states seriously suppress the degree of the resonance even if their potentials are weak. In the AG theory, the real part of the self-energy is usually neglected. In our theory, this approximation corresponds to an equation $s_2 = 0$. However s_2 plays an important role in the peak splitting. When we omit s_2 , I_2 and I_3 must be also zero, which leads to positive j and no splitting irrespective of $V_i N_0$ and $x_j k_F$.

We show that the impurity scattering causes the splitting of the ZBCP. The conclusions, however, do not deny a possibility of the BTRS. The appearance of the BTRS arises an important question whether the ZES is a stable state or not. Theoretical studies showed that the pair potential near the interface is suppressed when the ZES is formed at the interface^{23,26}. The ZES enhances the local density of states and therefore decreases the pair amplitude near the interface. Although d-wave pair potential is a source of the ZES, the ZES itself suppress the d-wave pair potential. The suppression of the d-wave component causes the subdominant or id wave component^{23,26}. If some subdominant pairing components always appear at the surface of superconductors, the ZES would be essentially an unstable state. At present, we have only limited information on the BTRS within the mean-field theories. To understand the nature of the

BTRSS further, we have to analyze electronic structure of high- T_c superconductors based on microscopic models and make clear effects of the surface, the electron correlation and the random potentials on the superconducting state. This is an important future problem.

Since the formation of the ZES is a universal phenomenon in superconductors with unconventional pairing symmetries, the ZES is also expected at a surface of spin-triplet superconductors⁶⁷. It is interesting to study effects of impurities on transport properties in spin-triplet superconductor junctions^{38,65,68,69,70,71,72,73,74,75,76,77,78,79,80}.

V. CONCLUSION

We show that the impurity scattering causes the split of the ZBCP in normal metal/d-wave superconductor junctions. The conductance is calculated from the Andreev and the normal reflection coefficients which are estimated by using the single-site approximation. We consider impurities near the junction interface on the superconductor side. The strength of the impurity scattering depends on the transparency of the junction (T_B), the position of impurities and the energy of a quasiparticle because the ZES are formed at the interface. The dip structure can be seen in the differential conductance when the bias-voltage is smaller than $E_{\text{dip}} = \epsilon_0 T_B = (\epsilon_0 k_F)^3$. In addition to the dip structure, we find the conductance peak for $E < E_{\text{ZEP}}$, where $E_{\text{ZEP}} = \epsilon_0 T_B$ is the width of the ZBCP in clean junctions. The results are consistent with previous numerical simulations. The present theory explains the two conductance shapes observed in experiments. We conclude that the split of the ZBCP in zero magnetic field is not the direct evidence of the broken time reversal symmetry states at a surface of a high- T_c superconductor.

APPENDIX A : TRANSMISSION AND REFLECTION COEFFICIENTS

In the clean NS junctions, the transmission and the reflection coefficients can be calculated from the appropriate boundary condition of the wave function. The calculated results are shown below.

$$r_{NN}^{he}(l) = \frac{k_1^2}{1} \frac{1}{2} e^{-i' \cdot l}; \quad (A 1)$$

$$r_{NN}^{ee}(l) = \frac{i z_0 (k_1 - i z_0)}{1} E; \quad (A 2)$$

$$t_{SN}^{ee}(l) = \frac{k_1 (k_1 - i z_0)}{1} E u_1 e^{-i' \cdot l}; \quad (A 3)$$

$$t_{SN}^{he}(l) = \frac{i z_0 k_1}{1} E v_1 e^{-i' \cdot l}; \quad (A 4)$$

$$r_{NN}^{hh}(l) = \frac{k_1^2}{1} \frac{1}{2} e^{i' \cdot l}; \quad (A 5)$$

$$r_{NN}^{hh}(l) = \frac{i z_0 (k_1 + i z_0)}{1} E; \quad (A 6)$$

$$t_{SN}^{hh}(l) = \frac{k_1 (k_1 + i z_0)}{1} E u_1 e^{i' \cdot l}; \quad (A 7)$$

$$t_{SN}^{hh}(l) = \frac{i z_0 k_1}{1} E v_1 e^{i' \cdot l}; \quad (A 8)$$

$$r_{SS}^{he}(l) = \frac{k_1^2 + 2z_0^2}{1} \frac{1}{2}; \quad (A 9)$$

$$r_{SS}^{ee}(l) = \frac{i z_0 (k_1 - i z_0)}{1}; \quad (A 10)$$

$$t_{NS}^{ee}(l) = \frac{k_1 (k_1 - i z_0)}{1} u_1 e^{i' \cdot l}; \quad (A 11)$$

$$t_{NS}^{he}(l) = \frac{i z_0 k_1}{1} v_1 e^{-i' \cdot l}; \quad (A 12)$$

(A 13)

$$r_{SS}^{hh}(l) = \frac{k_1^2 + 2z_0^2}{1} \frac{1}{2}; \quad (A 14)$$

$$r_{SS}^{hh}(l) = \frac{i z_0 (k_1 + i z_0)}{1}; \quad (A 15)$$

$$t_{NS}^{hh}(l) = \frac{k_1 (k_1 + i z_0)}{1} u_1 e^{i' \cdot l}; \quad (A 16)$$

$$t_{NS}^{hh}(l) = \frac{i z_0 k_1}{1} v_1 e^{-i' \cdot l}; \quad (A 17)$$

$$1 = E z_0^2 + k_1^2 \frac{E + 1}{2} : \quad (A 18)$$

For instance, $t_{NS}^{he}(l)$ is the transmission coefficient from the electron branch in a superconductor to the hole branch in a normal metal. In above coefficients, we use a relation $q_1 = k_1' \cdot k_1$ for simplicity. The conclusions in this paper remain unchanged in this approximation.

APPENDIX B : GREEN FUNCTIONS

The real space retarded Green function in clean junctions can be calculated by using the transmission and the reflection coefficients in Appendix A. For $x < x^0 < 0$, the Green function from a normal metal to a normal metal is

$$\hat{G}_0^{NN}(r; r^0) = \frac{iN_0}{W} \sum_{k_y^{(1)}} e^{ik_y^{(1)}(y - y^0)} \frac{1}{q^+} \begin{pmatrix} 1 & 0 \\ 0 & 0 \end{pmatrix} e^{iq_1^+ x - iq_1^+ x^0} j + \frac{0 & 0}{1 & 0} e^{iq_1^- x} e^{iq_1^+ x^0} r_{NN}^{he}(l) + \frac{1 & 0}{0 & 0} e^{iq_1^+ (x + x^0)} r_{NN}^{ee}(l) + \frac{1}{q} \begin{pmatrix} 0 & 0 \\ 0 & 1 \end{pmatrix} e^{iq_1^- x} e^{iq_1^+ x^0} r_{NN}^{eh}(l) + \frac{0 & 0}{0 & 0} e^{iq_1^- (x + x^0)} r_{NN}^{hh}(l) ; \quad (B1)$$

$$N_0 = \frac{m}{h^2} ; \quad (B2)$$

For $x > x^0 > 0$, the Green function from a superconductor to a superconductor is

$$\hat{G}_0^{SS}(r; r^0) = \frac{iN_0}{W} \sum_{k_y^{(1)}} e^{ik_y^{(1)}(y - y^0)} \frac{E}{1} \wedge \frac{1}{k^+} \begin{pmatrix} u_1^2 & u_1 v_1 \\ u_1 v_1 & v_1^2 \end{pmatrix} e^{ik_1^+ x - iq_1^+ x^0} j + \frac{u_1 v_1}{u_1^2} \begin{pmatrix} v_1^2 \\ u_1 v_1 \end{pmatrix} e^{ik_1^- x + ik_1^+ x^0} r_{SS}^{he}(l) + \frac{u_1^2}{u_1 v_1} \begin{pmatrix} u_1 v_1 \\ v_1^2 \end{pmatrix} e^{ik_1^+ (x + x^0)} r_{SS}^{ee}(l) + \frac{1}{k} \begin{pmatrix} v_1^2 \\ u_1 v_1 \end{pmatrix} \begin{pmatrix} u_1 v_1 \\ u_1^2 \end{pmatrix} e^{ik_1^- x - ik_1^+ x^0} r_{SS}^{eh}(l) + \frac{v_1^2}{u_1 v_1} \begin{pmatrix} u_1 v_1 \\ u_1^2 \end{pmatrix} e^{ik_1^- (x + x^0)} r_{SS}^{hh}(l) \wedge ; \quad (B3)$$

$$\wedge = \begin{pmatrix} e^{i\frac{\pi}{2}} & 0 \\ 0 & e^{-i\frac{\pi}{2}} \end{pmatrix} ; \quad (B4)$$

where \wedge is the phase of a superconductor. For $x > 0 > x^0$, the Green function from a normal metal to a superconductor is

$$\hat{G}_0^{SN}(r; r^0) = \frac{iN_0}{W} \sum_{k_y^{(1)}} e^{ik_y^{(1)}(y - y^0)} \wedge \frac{1}{q^+} \begin{pmatrix} u_1 & 0 \\ v_1 & 0 \end{pmatrix} e^{ik_1^+ x - iq_1^+ x^0} t_{SN}^{ee}(l) + \frac{v_1 & 0}{u_1 & 0} e^{ik_1^- x - iq_1^+ x^0} t_{SN}^{he}(l) + \frac{1}{q} \begin{pmatrix} 0 & v_1 \\ 0 & u_1 \end{pmatrix} e^{ik_1^- x + iq_1^+ x^0} t_{SN}^{hh}(l) + \frac{0 & u_1}{0 & v_1} e^{ik_1^+ x + iq_1^+ x^0} t_{SN}^{eh}(l) : \quad (B5)$$

For $x < 0 < x^0$, the Green function from a superconductor to a normal metal is

$$\hat{G}_0^{NS}(r; r^0) = \frac{iN_0}{W} \sum_{k_y^{(1)}} e^{ik_y^{(1)}(y - y^0)} \frac{E}{1} \frac{1}{k^+} \begin{pmatrix} u_1 & v_1 \\ 0 & 0 \end{pmatrix} e^{iq_1^+ x + ik_1^+ x^0} t_{NS}^{ee}(l) + \frac{0 & 0}{u_1 & v_1} e^{iq_1^- x + ik_1^+ x^0} t_{NS}^{he}(l) + \frac{1}{k} \begin{pmatrix} 0 & 0 \\ v_1 & u_1 \end{pmatrix} e^{iq_1^- x - ik_1^+ x^0} t_{NS}^{hh}(l) + \frac{v_1 & u_1}{0 & 0} e^{iq_1^+ x - ik_1^+ x^0} t_{NS}^{eh}(l) \wedge : \quad (B6)$$

¹ Electronic address: asano@eng.hokudai.ac.jp
¹ C.R.Hu, Phys. Rev. Lett. 72, 1526 (1994).

² S. Kashiwaya and Y. Tanaka, Rep. Prog. Phys. 63, 1641 (2001).

³ Y. Tanaka and S. Kashiwaya, *Phys. Rev. Lett.* **74**, 3451 (1995).

⁴ S. Kashiwaya, Y. Tanaka, M. Koyanagi, H. Takashima, and K. Kajimura, *Phys. Rev. B* **51**, 1350 (1995).

⁵ L. Al, H. Takashima, S. Kashiwaya, N. Terada, H. Ihara, Y. Tanaka, M. Koyanagi, and K. Kajimura, *Phys. Rev. B* **55**, 14757 (1997).

⁶ W. Wang, M. Yamazaki, K. Lee, and I. Iguchi, *Phys. Rev. B* **60**, 4272 (1999).

⁷ J. Y. T. Wei, N.-C. Yeh, D. F. Garrigus, and M. Strasik, *Phys. Rev. Lett.* **81**, 2542 (1998).

⁸ I. Iguchi, W. Wang, M. Yamazaki, Y. Tanaka, and S. Kashiwaya, *Phys. Rev. B* **62**, R6131 (2000).

⁹ J. Geerk, X. X. Xi, and G. Linker, *Z. Phys. B* **73**, 329 (1988).

¹⁰ Z. Q. Mao, M. M. Rosario, K. D. Nelson, K. Wu, I. G. Deac, P. Schierer, Y. Liu, T. He, K. A. Regan, and R. J. Cava, *Phys. Rev. B* **67**, 094502 (2003).

¹¹ Y. S. Barash, H. Burkhardt, and D. Rainer, *Phys. Rev. Lett.* **77**, 4070 (1996).

¹² Y. Tanaka and S. Kashiwaya, *Phys. Rev. B* **53**, R11957 (1996).

¹³ Y. Tanaka and S. Kashiwaya, *Phys. Rev. B* **56**, 892 (1997).

¹⁴ Y. Tanaka and S. Kashiwaya, *Phys. Rev. B* **58**, R2948 (1998).

¹⁵ Y. Tanaka and S. Kashiwaya, *J. Phys. Soc. Jpn.* **68**, 3485 (1999); *J. Phys. Soc. Jpn.* **69**, 1152 (2000).

¹⁶ Y. A. Sano, *Phys. Rev. B* **64**, 224515 (2001).

¹⁷ A. F. Andreev, *Zh. Eksp. Teor. Fiz.* **46**, 1823 (1964) [Sov. Phys. JETP **19**, 1228 (1964)].

¹⁸ M. Fogelstrom, D. Rainer, and J. A. Sauls, *Phys. Rev. Lett.* **79**, 281 (1997); D. Rainer, H. Burkhardt, M. Fogelstrom, and J. A. Sauls, *J. Phys. Chem. Solids* **59**, 2040 (1998).

¹⁹ Y. Tanaka, H. Tsuchiura, Y. Tanuma, and S. Kashiwaya, *J. Phys. Soc. Jpn.* **71**, 271 (2002).

²⁰ Y. Tanaka, H. Itoh, H. Tsuchiura, Y. Tanuma, J. Inoue, and S. Kashiwaya, *J. Phys. Soc. Jpn.* **71**, 2005 (2002).

²¹ Y. Tanaka, Y. Tanuma, K. Kuroki, and S. Kashiwaya, *J. Phys. Soc. Jpn.* **71**, 2102 (2002).

²² S. Kashiwaya, Y. Tanaka, M. Koyanagi, and K. Kajimura, *J. Phys. Chem. Solids* **56**, 1721 (1995).

²³ M. Matsumoto and H. Shiba, *J. Phys. Soc. Jpn.* **64**, 4867 (1995).

²⁴ Y. Tanuma, Y. Tanaka, M. Ogata, and S. Kashiwaya, *J. Phys. Soc. Jpn.* **67**, 1118 (1998).

²⁵ Y. Tanuma, Y. Tanaka, M. Ogata, and S. Kashiwaya, *Phys. Rev. B* **60**, 9817 (1999).

²⁶ Y. Tanuma, Y. Tanaka, and S. Kashiwaya, *Phys. Rev. B* **64**, 214519 (2001).

²⁷ I. Lubinova and G. Koren, cond-mat/0306030.

²⁸ N. Kitaura, H. Itoh, Y. A. Sano, Y. Tanaka, J. Inoue, Y. Tanuma, and S. Kashiwaya, *J. Phys. Soc. Jpn.* **72**, (2003) in press.

²⁹ R. B. Laughlin, *Phys. Rev. Lett.* **80**, 5188 (1998).

³⁰ M. Covington, M. Aprili, E. Paraoanu, L. H. Gurene, F. Xu, J. Zhu, and C. A. Mirkin, *Phys. Rev. Lett.* **79**, 277 (1997).

³¹ A. Biswas, P. Fournier, M. M. Qazilbash, V. N. Smolyaninova, H. Balci, and R. L. Greene, *Phys. Rev. Lett.* **88**, 207004 (2002).

³² Y. Dagan and G. Deutscher, *Phys. Rev. Lett.* **87**, 177004 (2001).

³³ A. Sharoni, O. Millo, A. Kohen, Y. Dagan, R. Beck, G. Deutscher, and G. Koren, *Phys. Rev. B* **65**, 134526 (2002).

³⁴ A. Kohen, G. Leibovitch, and G. Deutscher, *Phys. Rev. Lett.* **90**, 207005 (2003).

³⁵ J. W. Ekin, Y. Xu, S. Mao, T. Venkatesan, D. W. Face, M. Eddy, and S. A. Wolf, *Phys. Rev. B* **56**, 13746 (1997).

³⁶ A. Sawa, S. Kashiwaya, H. Obara, H. Yamazaki, M. Koyanagi, Y. Tanaka, and N. Yoshida, *Physica C* **339**, 107 (2000).

³⁷ H. Aubin, L. H. Greene, S. Jian, and D. G. Hinks, *Phys. Rev. Lett.* **89**, 177001 (2002).

³⁸ T. Hirai, Y. Tanaka, N. Yoshida, Y. A. Sano, J. Inoue, and S. Kashiwaya, *Phys. Rev. B* **67**, 174501 (2003).

³⁹ N. Yoshida, Y. A. Sano, H. Itoh, Y. Tanaka, and J. Inoue, *J. Phys. Soc. Jpn.* **72**, 895 (2003).

⁴⁰ Y. A. Sano and Y. Tanaka, *Phys. Rev. B* **65**, 064522 (2002).

⁴¹ Y. A. Sano, *Phys. Rev. B* **63**, 052512 (2001).

⁴² Y. A. Sano and Y. Tanaka, "Toward the controllable Quantum State" Eds. H. Takayanagi and J. Nitta, pp 185 (World Scientific, Singapore, 2003).

⁴³ Y. S. Barash, A. A. Svidzinsky, and H. Burkhardt, *Phys. Rev. B* **55**, 15282 (1997).

⁴⁴ A. A. Golubov and M. Y. Kupriyanov, *Pis'ma Zh. Eksp. Teor. z* **69**, 242 (1999) [Sov. Phys. JETP Lett. **69**, 262 (1999)]; **67**, 478 (1998) [Sov. Phys. JETP Lett. **67**, 501 (1998)].

⁴⁵ A. Poenische, Yu. S. Barash, C. Bruder, and V. Istyukov, *Phys. Rev. B* **59**, 7102 (1999).

⁴⁶ K. Yamada, Y. Nagato, S. Higashitani, and K. Nagai, *J. Phys. Soc. Jpn.* **65**, 1540 (1996).

⁴⁷ Y. Tanaka, Y. Tanuma, and S. Kashiwaya, *Phys. Rev. B* **64**, 054510 (2001).

⁴⁸ T. Luck, U. Eckem, and A. Shelankov, *Phys. Rev. B* **63**, 064510 (2001).

⁴⁹ G. Eilenberger, *Z. Phys.* **214**, 195 (1968).

⁵⁰ A. I. Larkin and Yu. N. Ovchinnikov, *Eksp. Teor. Fiz.* **55**, 2262 (1986) [Sov. Phys. JETP **28**, 1200 (1968)].

⁵¹ A. V. Zaitsev, *Zh. Eksp. Teor. Fiz.* **86**, 1742 (1984) [Sov. Phys. JETP **59**, 1015 (1984)].

⁵² A. L. Schelankov, *J. Low. Temp. Phys.* **60**, 29 (1985).

⁵³ C. Bruder, *Phys. Rev. B* **41**, 4017 (1990).

⁵⁴ P. A. Lee and D. S. Fisher, *Phys. Rev. Lett.* **47**, 882 (1981).

⁵⁵ G. E. Blonder, M. Tinkham, and T. M. Klapwijk, *Phys. Rev. B* **25**, 4515 (1982).

⁵⁶ Y. Takane and H. Ebisawa, *J. Phys. Soc. Jpn.* **61**, 1685 (1992).

⁵⁷ P. G. de Gennes, *Superconductivity of Metals and Alloys*, (Benjamin, New York, 1966).

⁵⁸ Y. Tanaka, T. Asai, N. Yoshida, J. Inoue, and S. Kashiwaya, *Phys. Rev. B* **61**, R11902 (2000).

⁵⁹ Y. A. Sano and G. E. W. Bauer, *Phys. Rev. B* **54**, 11602 (1996); Erratum **54**, 9972 (1997).

⁶⁰ Y. Tanaka and S. Kashiwaya, *Phys. Rev. B* **53**, 9371 (1996).

⁶¹ M. Matsumoto and H. Shiba, *J. Phys. Soc. Jpn.* **64**, 1703 (1995).

⁶² M. Aprili, M. Covington, E. Paraoanu, B. Niedermeyer, and L. H. Greene, *Phys. Rev. B* **57**, R8139 (1998).

⁶³ Y. Tanaka, Yu. Nazarov, and S. Kashiwaya, *Phys. Rev. Lett.* **90**, 167003 (2003).

⁶⁴ Y. A. Sano, *Phys. Rev. B* **64**, 014511 (2001).

⁶⁵ Y. A. Sano, *J. Phys. Soc. Jpn.* **71**, 905 (2002).

⁶⁶ A. A. Abrikosov, L. P. Gor'kov, and I. E. Dzyaloshinskii, *Quantum Field Theoretical Methods in Statistical Physics*,

(Pergamon Press, London, 1963).

⁶⁷ L. J. Buchholtz and G. Zwicknagl, Phys. Rev. B 23, 5788 (1981).

⁶⁸ M. Yamashiro, Y. Tanaka, and S. Kashiwaya, Phys. Rev. B 56, 7847 (1997).

⁶⁹ M. Yamashiro, Y. Tanaka, Y. Tanum a, and S. Kashiwaya, J. Phys. Soc. Jpn. 67, 3224 (1998).

⁷⁰ M. Yamashiro, Y. Tanaka, N. Yoshida, and S. Kashiwaya, J. Phys. Soc. Jpn. 68, 2019 (1999).

⁷¹ N. Yoshida, Y. Tanaka, J. Inoue, and S. Kashiwaya, J. Phys. Soc. Jpn. 68, 1071 (1999).

⁷² T. Hirai, N. Yoshida, Y. Tanaka, J. Inoue, and S. Kashiwaya, J. Phys. Soc. Jpn. 70, 1885 (2001).

⁷³ Y. Tanum a, K. Kuroki, Y. Tanaka, and S. Kashiwaya, Phys. Rev. B 64, 214510 (2001).

⁷⁴ Y. Tanum a, K. Kuroki, Y. Tanaka, R. Arita, S. Kashiwaya, and H. Aoki, Phys. Rev. B 65, 064522 (2002).

⁷⁵ Y. Tanaka, T. Hirai, K. Kusakabe, and S. Kashiwaya, Phys. Rev. B 60, 6308 (1999).

⁷⁶ C. Honerkamp and M. Sigrist, J. Low. Temp. Phys. 111, 898 (1998); Prog. Theor. Phys. 100, 53 (1998).

⁷⁷ N. Stefanakis, Phys. Rev. B 64, 224502 (2001); J. Phys. Cond. Matt. 13, 3643 (2001).

⁷⁸ K. Sengupta, I. Zutic, H.-J. Kwon, V. M. Yakovenko, and S. Das Sarma, Phys. Rev. B 63, 144531 (2001).

⁷⁹ Y. Asano and K. Katabuchi, J. Phys. Soc. Jpn. 71, 1974 (2002).

⁸⁰ Y. Asano, Y. Tanaka, M. Sigrist, and S. Kashiwaya, Phys. Rev. B 67, 184505 (2003).